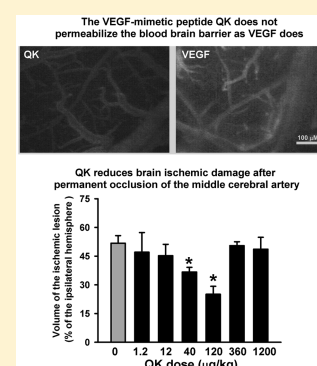


Neuroprotective Effect of VEGF-Mimetic Peptide QK in Experimental Brain Ischemia Induced in Rat by Middle Cerebral Artery Occlusion

Giuseppe Pignataro,[†] Barbara Ziaco,[§] Anna Tortiglione,[†] Rosaria Gala,[†] Ornella Cuomo,[†] Antonio Vinciguerra,[†] Dominga Lapi,[‡] Teresa Mastantuono,[‡] Serenella Anzilotti,^{||} Luca Domenico D'Andrea,[§] Carlo Pedone,[§] Gianfranco di Renzo,[†] Lucio Annunziato,^{†,||} and Mauro Cataldi^{*,†}[†]Division of Pharmacology, Department of Neuroscience, Reproductive and Odontostomatologic Sciences, [‡]Division of Physiology, Department of Clinical Medicine and Surgery, School of Medicine, Federico II University of Naples, 80131 Naples, Italy[§]Institute of Biostructure and Bioimaging, Italian National Research Council (CNR), 80145 Naples, Italy^{||}IRCCS SDN, Via Gianturco, 80143 Naples, Italy

ABSTRACT: We investigated the effect of the VEGF-mimetic peptide, QK, on ischemic brain damage and on blood–brain barrier permeability in the rat. QK administered by the intracerebroventricular, intravenous, or intranasal route caused a 40% decrease in ischemic brain damage induced by permanent occlusion of the middle cerebral artery relative to that in controls. No increase in the volume of the ischemic hemisphere compared to that of the contralateral nonischemic hemisphere was observed in rats treated with QK, suggesting that this peptide did not cause brain edema. The effect of QK on vessel permeability was evaluated by intravital pial microvessel videomaging, a technique that allows the pial vessels to be visualized through a surgically prepared open cranial window. The results showed that QK did not cause any leakage of intravenously injected fluorescein–dextran conjugates after intracarotid administration or topical application to the brain cortex. Collectively, these data suggest that QK may exert neuroprotective activity in the context of stroke without promoting any increase in vascular permeability. Because VEGF's neuroprotective activity may be overshadowed by the appearance of brain edema and microbleeds, QK could represent a significant step forward in stroke treatment.

KEYWORDS: Cerebral ischemia, vascular endothelial growth factor, vascular permeability, brain edema, neuroprotection



VEGF has long been considered a promising drug candidate for stroke therapy because of its neuroregenerative and neuroprotective properties.¹ Indeed, after a stroke, the synthesis and release of VEGF are induced in the brain,² and this growth factor orchestrates a reparative cascade that aims to restore blood perfusion through new blood vessels and to repopulate the injured brain with new neuronal, glial, and endothelial cells.^{3,4} Specifically, VEGF activates the neurovascular niche, a highly specialized unit composed of mutually interacting neuroblasts and newly formed endothelial cells and glial cells.^{1,5–7} Moreover, VEGF exerts significant neuroprotective activity in *in vitro* models of ischemic neuronal cell death⁸ and excitotoxicity.^{9,10} This suggests that, after stroke, VEGF not only promotes regeneration but also rescues neurons in the ischemic penumbra,¹¹ the brain region that surrounds the ischemic core and that dies hours or days after vessel occlusion because of the impairment of intracellular ion homeostasis.^{12–14}

Despite this strong rationale, the use of VEGF in experimental brain ischemia has yielded controversial and generally disappointing results. It has become clear that the increase in vascular permeability induced by this growth factor may overshadow its neuroprotective effects.^{15,16} VEGF induces, indeed, the formation of blood vessels that are immature and

leaky¹⁷ and acutely increases the permeability of preexisting blood vessels, causing the loosening of endothelial cell junctions and the formation of fenestrations.^{18–22} Because of these effects on vascular permeability, VEGF caused brain edema and microbleeds and ultimately worsened tissue damage in animal models of stroke.^{23,24} Therefore, the development of this growth factor as a therapeutic tool in brain ischemia appears to be problematic.

New VEGF-like peptides with proangiogenic activity have been recently synthesized. They are considered to be a promising alternative to VEGF for clinical applications such as wound repair and ulcer healing because of their less expensive and easier synthesis.^{25,26} It is still unclear, however, whether these VEGF-mimetic peptides could also represent an improvement over VEGF for stroke therapy. In particular, it has not yet been established whether they have neuroprotective activity in the context of stroke and whether they promote blood–brain barrier (BBB) permeabilization like VEGF. In the present article, we explored this issue using one of the most interesting members of this new family of VEGF-mimetic peptides, the QK peptide that

Received: October 6, 2014

Published: July 14, 2015

was originally synthesized in our laboratories.²⁷ QK reproduces, in a stable form, the helix conformation of VEGF residues 17–25, which represents one of the regions of this growth factor that take part in the recognition of VEGF receptors.^{28,29} This peptide, which is remarkably stable in serum,³⁰ activates VEGF receptors²⁷ and induces angiogenesis both *in vitro*³⁰ and *in vivo*.^{31,32} In addition, QK decreases neuronal cell damage in different experimental models of peripheral neuropathy, suggesting that it could also have neuroprotective activity.³³ Here, we show that, in rats, QK administered either by the intracerebroventricular (icv), intravenous (iv), or intranasal route reduced brain damage in experimental brain ischemia induced by the permanent occlusion of the middle cerebral artery (pMCAO). Unlike VEGF, QK did not promote BBB permeabilization, as evaluated by intravital pial microvessel videomaging.

RESULTS AND DISCUSSION

QK Decreases pMCAO-Induced Ischemic Brain Damage. To establish whether QK has neuroprotective properties in brain ischemia induced by pMCAO, we first evaluated its effect after icv administration because this route enables direct drug delivery into the brain. As detailed in the **Methods**, peptide administration began at the time that the QK-containing osmotic minipump was implanted (releasing 3 $\mu\text{g}/\text{mL}$ QK at a rate of 1 $\mu\text{L}/\text{h}$), 30 min before the induction of brain ischemia. The percent of ischemic brain damage evaluated 3 days after pMCAO was significantly lower in rats icv-injected with QK ($n = 7$) as compared with that in control animals that received normal saline by the same route of administration (Figure 1A). These

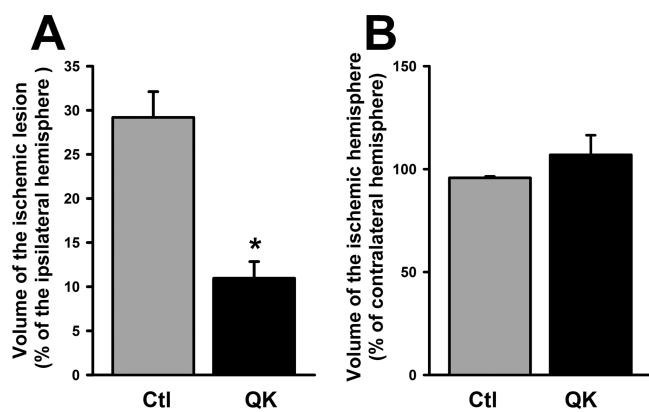


Figure 1. Intracerebroventricularly injected QK reduces ischemic brain damage. (A) Ischemic brain damage, expressed as a percent of the total volume of the ipsilateral brain hemisphere, in rats implanted with a QK- (3 $\mu\text{g}/\text{mL}$, 1 $\mu\text{L}/\text{h}$) or vehicle-containing Alzet osmotic minipump, implanted 30 min before pMCAO, and sacrificed 72 h later. (B) Percent ratio between the volumes of the hemispheres ipsi- and contralateral to pMCAO in the same experimental groups in panel A. * $p < 0.05$ vs control (Mann–Whitney test).

results showed that icv-injected QK elicits neuroprotection in the context of stroke. The percent ratio of the volumes of the ischemic and contralateral hemispheres was close to 100% in both QK- and vehicle-injected rats, suggesting that QK did not promote brain edema (Figure 1B).

The icv route is highly invasive and, hence, not amenable for possible clinical development. Therefore, we investigated whether QK was still effective when given by the less invasive iv route. Preliminary experiments were performed to assess

whether QK may cross the BBB. To this end, we used intravital pial microvessel videomaging, a technique based on the visualization of pial microvessels through a window drilled in the skull. Specifically, we looked for the appearance of fluorescence in brain vessels and parenchyma after the injection of fluorescein-conjugated QK (50 $\mu\text{g}/\text{kg}$, in three consecutive boluses, $n = 4$) into the internal carotid artery. The results showed the appearance of bright fluorescence first in the arteriolar and then in the venular compartment (Figure 2A–C).

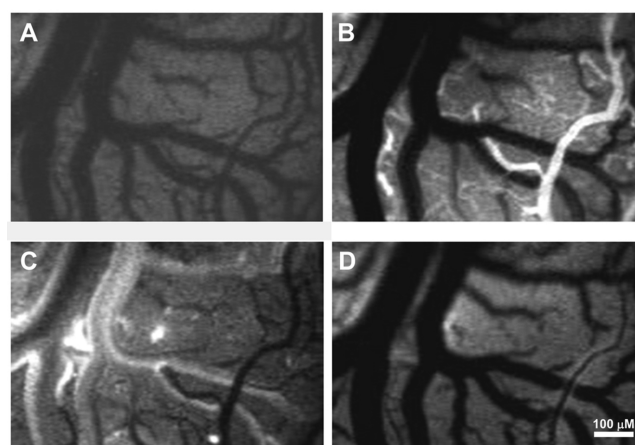


Figure 2. Time course of pial vessel visualization after intracarotid injection of fluorescein-conjugated QK. The four panels show images of the pial circulation visualized through a transcranial window that were taken before (A) and 20 s (B), 28 s (C), and 40 s (D) after the intracarotid injection of QK (120 $\mu\text{g}/\text{kg}$ in three consecutive boluses) in an anesthetized rat representative of a group of 4. Note the rapid appearance of bright fluorescence in the arteriolar compartment (B) and the later visualization of the venular compartment in panel C. The image in panel D shows that diffuse fluorescence can be observed in the brain parenchyma even when fluorescence is no longer apparent in the vessel lumina. This suggested that some fluorescent QK crossed the vessel wall and entered the brain.

Thereafter, fluorescent QK adhered to the vessel wall and extravasated in the brain parenchyma, as shown by the progressive increase in interstitial fluorescence on the venular side up to values 10-fold higher than baseline by 3 \pm 1 min after injection (NGL values: 0.21 \pm 0.04 vs 0.02 \pm 0.01, $p < 0.01$) (Figures 2D and 3). Similar results were obtained after iv injection of fluorescent QK, although, as expected, higher doses were needed and fluorescence was fainter than that after intracarotid injection (Figure 4). These data indicated that QK may cross the BBB and reach the brain parenchyma.

To establish whether intravenous QK could exert neuroprotective activity in the context of stroke once it enters the brain, we compared the ischemic brain damage induced by pMCAO in seven different groups of rats that were injected 1 h after pMCAO either with this peptide at doses of 1.2, 12, 40, 120, 360, and 1200 $\mu\text{g}/\text{kg}$ or with its vehicle. Ischemic damage measured 3 days after pMCAO was significantly lower in rats receiving 40 or 120 $\mu\text{g}/\text{kg}$ QK ($n = 5$ and 6, respectively) than in those injected with vehicle ($n = 5$) or lower QK doses. Interestingly, no neuroprotection was observed in rats receiving the higher doses of 360 and 1200 $\mu\text{g}/\text{kg}$ (Figure 5A). Similar to observations with icv-administered QK, iv-administered QK did not increase the percent ratio of the volumes of the ischemic and contralateral hemispheres, which was close to 100% in treated animals and controls (Figure 5B). This suggested that iv QK did not induce brain edema.

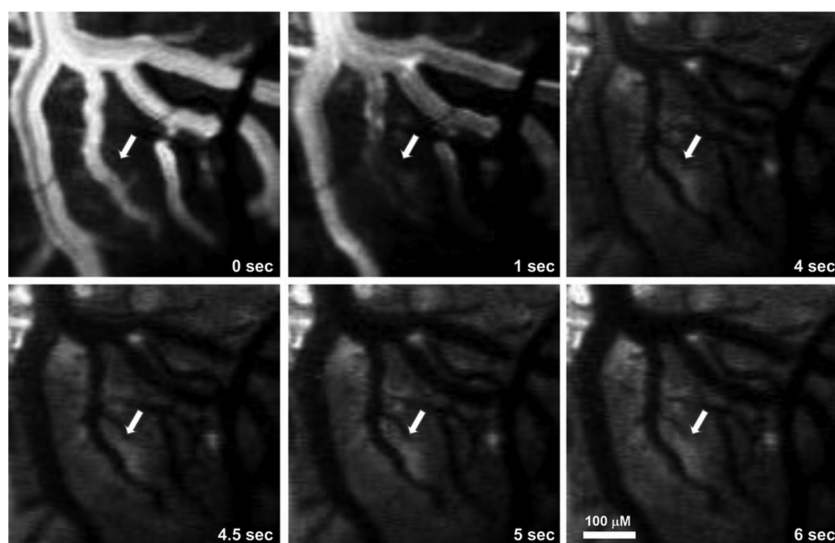


Figure 3. Fluorescein-conjugated QK adheres to the vessel wall and extravasates into the brain parenchyma. Images are shown of a portion of the microscopic field reproduced in Figure 2, taken at a shortened time interval to illustrate in more detail the kinetics of QK extravasation into the brain parenchyma. The time elapsed is based on the appearance of fluorescence in the arteriole indicated by the arrows. Although QK fluorescence was no longer appreciable in the lumen of the arteriole by 1 s from the time of its initial visualization, the fluorescence gradually diffused into the surrounding brain parenchyma over the following 5 s.

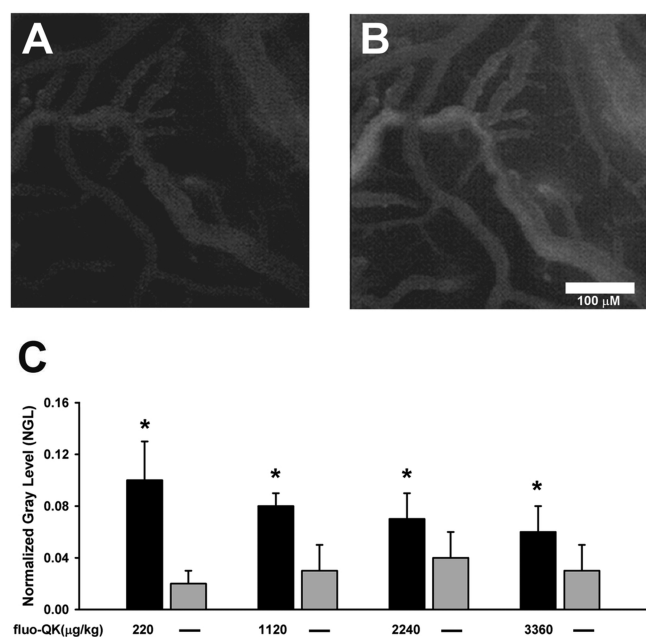


Figure 4. Changes in pial vessel fluorescence after injection of fluorescein-conjugated QK. (A, B) Images of the same field before and 5 min after iv injection of 1120 $\mu\text{g}/\text{kg}$ fluorescein-conjugated QK. Note that a slight but distinct increase in fluorescence occurred in both the vessel lumina and brain parenchyma after peptide injection. (C) NGL values measured after the injection of vehicle (gray bars) or increasing doses of fluorescent QK (black bars). For each dose, the plot shows the mean \pm SEM of the values obtained from five different animals. * $p < 0.05$ vs control.

A significant improvement in general neurological scores was observed in rats receiving 120 $\mu\text{g}/\text{kg}$ QK and in focal scores in those treated with 40, 120, or 360 $\mu\text{g}/\text{kg}$ QK (Figure 5C,D).

Collectively, these data provided a proof of concept that the small VEGF-mimetic peptide, QK, may exert a neuroprotective effect in the context of stroke.

QK May Be Administered Intranasally To Elicit Neuroprotection in Stroke.

During a stroke, a short delay between the beginning of symptoms and the institution of treatment is essential to rescue the ischemic brain from death. Therefore, great efforts are currently directed to develop modalities of drug administration that could help to institute pharmacological treatment even before the patient is admitted to the stroke unit. An interesting possibility to achieve this goal is to give neuroprotective drugs by the intranasal route. Drugs administered by this route gain direct access to the brain, bypassing the BBB because they diffuse along the olfactory and trigeminal fibers^{34,35} and spreading to very far regions, including those that are more severely damaged in stroke, such as the cortex and striatum. Intranasal administration is considered to be a promising strategy to deliver growth factors such as IGF-1, erythropoietin, NGF, TGF- β , and VEGF to the brain for the treatment of neurodegenerative diseases.^{35–43} Therefore, we investigated whether QK-induced neuroprotection was still observed when this peptide was given intranasally. We first examined whether intranasally administered QK could gain access to the brain. To this end, we instilled a fluorescein-QK conjugate into the nostrils of nonischemic rats and looked for the appearance of fluorescence in different brain regions 3 h thereafter. Confocal microscopy experiments showed bright fluorescence in the cerebellar cortex, hippocampus, striatum, and olfactory bulbs, whereas the signal was faint in the cerebral cortex (Figure 6). These results suggested that QK diffused into the brain after intranasal administration. The strong fluorescence that we observed in the olfactory bulbs and cerebellum was not unexpected because similar results have been reported with other fluorescent peptides and with living cells given by the intranasal route. The preferential distribution of intranasally administered compounds to these brain regions could be explained by their diffusion along the olfactory and trigeminal neural pathways.⁴⁴

To establish whether intranasal QK exerted a neuroprotective effect in the context of stroke, we instilled QK (12 $\mu\text{g}/\text{kg}$ in 5 aliquots of 10 μL given alternatively in the two nostrils in a single session, $n = 7$) or its vehicle ($n = 7$) in the nostrils of pMCAO-

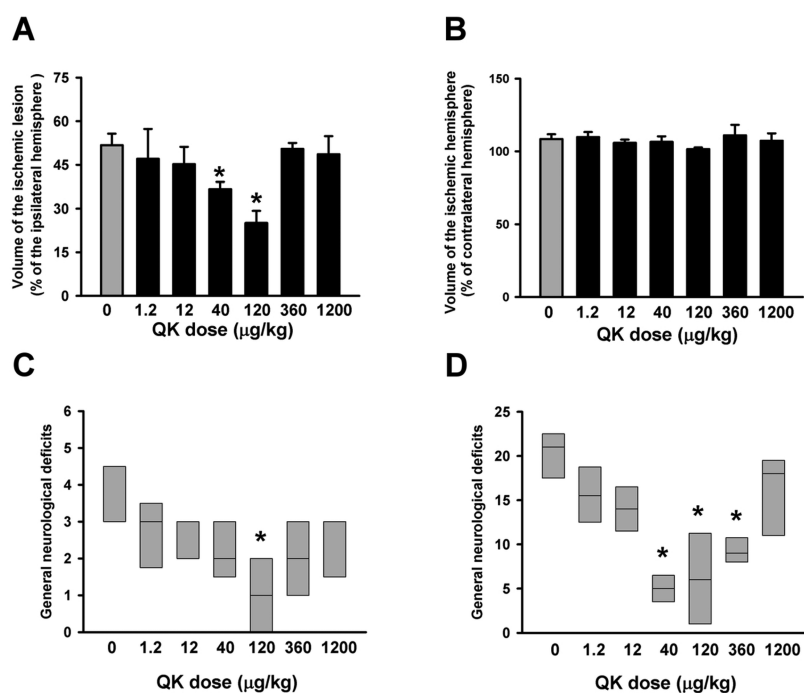


Figure 5. Intravenously injected QK reduces ischemic brain damage. (A) Ischemic brain damage, expressed as a percent of the total volume of the ipsilateral brain hemisphere, in rats injected with QK (1.2–1200 $\mu\text{g}/\text{kg}$) or its vehicle 1 h after pMCAO and sacrificed 3 days later. (B) Percent ratio between the volumes of the hemispheres ipsi- and contralateral to pMCAO in the same experimental groups in panel A. (C, D) Box plots of the general and focal neurological deficits expressed as Clark's scores, respectively. The data in panels A and B represent the mean + SEM of the values obtained in six different rats in the QK groups and in five in the control groups. * $p < 0.05$ vs control (ANOVA followed by Bonferroni's *posthoc* test in panels A and B; Kruskal–Wallis nonparametric ANOVA in panels C and D).

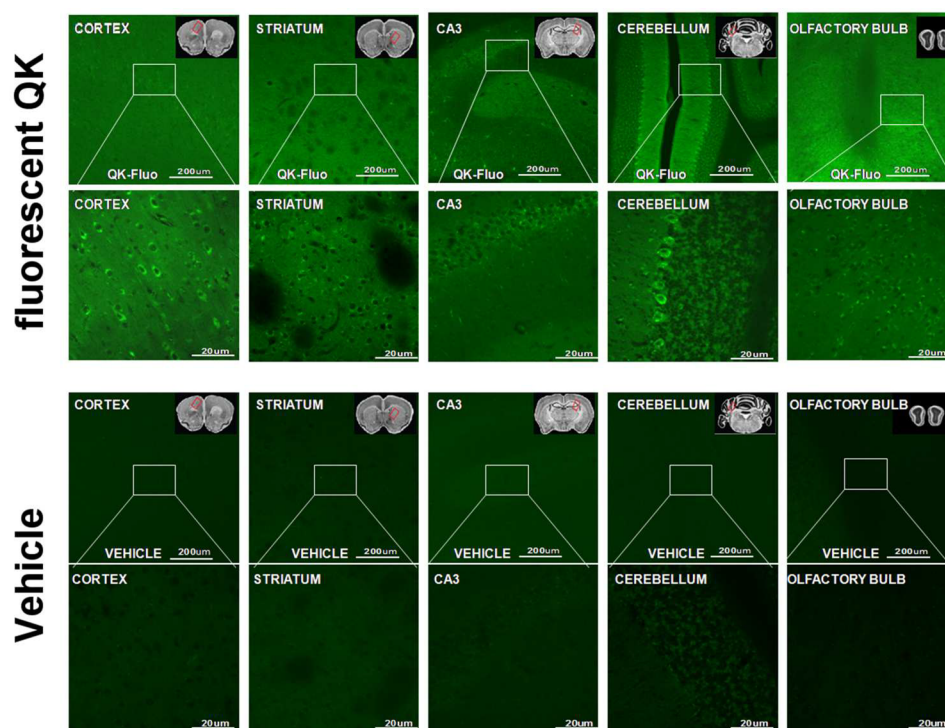


Figure 6. Intranasally instilled QK diffuses into the brain. Confocal images of coronal brain sections of rats sacrificed 3 h after the intranasal administration of 50 μL of a 75 $\mu\text{g}/\text{mL}$ solution of fluorescent QK (top two rows) or its vehicle (bottom two rows). In both groups, low- and high-magnification images from the cortex, striatum, hippocampus CA3 region, cerebellum, and olfactory bulb are reported as indicated. Note the very strong signal in the cerebellum, the moderate intensity of staining in the striatum and hippocampus CA3 subfield, and the weak fluorescence in the cortex. Note also that fluorescent QK decorates the surface of neurons in high-magnification images, suggesting a specific interaction of QK with plasmamembrane receptors.

induced rats 3 h after surgery. The ischemic damage evaluated 3 days after pMCAO was approximately 40% lower in rats receiving intranasal QK than that in controls ($n = 7$) (Figure 7A). A similar 40% neuroprotection was also observed in a group

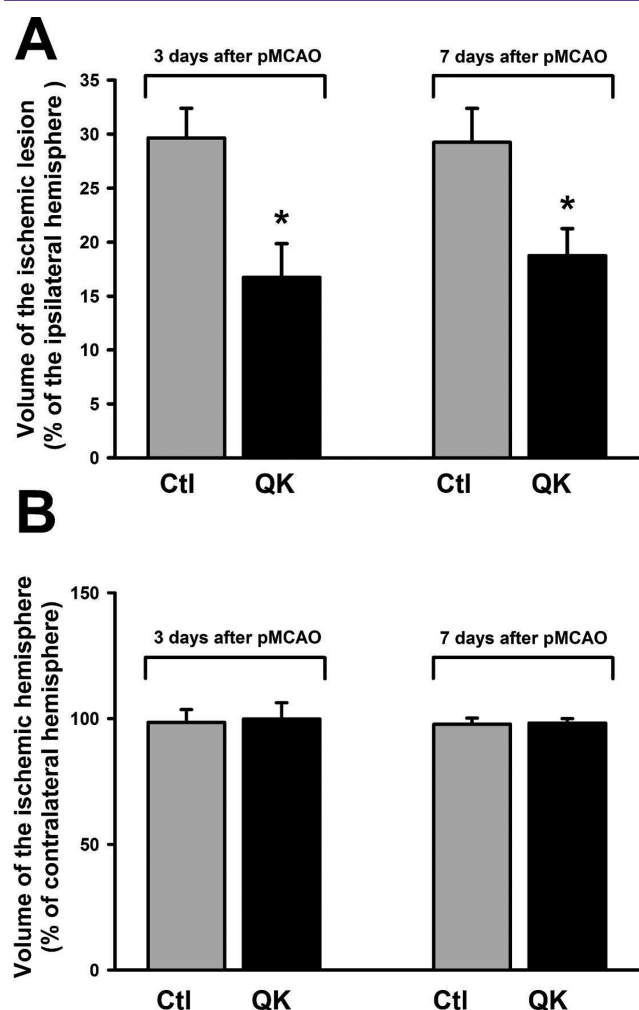


Figure 7. Intranasally instilled QK reduces ischemic brain damage. (A) Ischemic brain damage, expressed as a percent of the total volume of the ipsilateral brain hemisphere, in rats receiving intranasal QK (12 $\mu\text{g}/\text{kg}$) or its vehicle 3 h after pMCAO and sacrificed 3 or 7 days later, as indicated. (B) Ischemic brain edema evaluated as the percent ratio between the volumes of the hemispheres ipsi- and contralateral to pMCAO in the same experimental groups in panel A. * $p < 0.05$ vs control (Student's t test for unpaired data).

of rats sacrificed 7 days after QK ($n = 7$) intranasal administration compared to that of vehicle-treated controls ($n = 7$), suggesting that the effect of intranasally administering a single dose of QK persisted for at least a week (Figure 7A), a time point that was chosen because previous studies suggested that brain ischemic lesions become stable after this time and do not further progress.^{45,46} Interestingly, intranasal QK was effective at a dosage 10 times lower than the intravenous neuroprotective dose. This result could be explained by the fact that intranasally administered drugs bypass systemic distribution and clearance and thus reach higher concentrations in the brain than do comparable doses given intravenously.

In control and QK-treated rats sacrificed 3 or 7 days after pMCAO, the percent ratio of the volumes of the ischemic and contralateral hemispheres ranged around 100%, suggesting that,

like iv- or icv-administered QK, intranasally administered QK did not induce the formation of brain edema (Figure 7B).

QK Does Not Increase BBB Permeability. To investigate whether QK, like VEGF, may increase BBB permeability, we studied its effect on brain microvessels by intravital pial microvessel videoimaging. More specifically, we evaluated whether QK promoted the extravasation of fluorescent dextran into the brain parenchyma, a high-molecular-weight compound that does not cross the BBB under physiological conditions. Fluorescent dextran was injected through an indwelling femoral catheter, and parenchymal brain fluorescence beneath the cranial window was measured before and after the injection of either VEGF (28–84 $\mu\text{g}/\text{kg}$) or QK (1.2–220 $\mu\text{g}/\text{kg}$) in three consecutive boluses through the carotid artery. At all of the doses tested, parenchymal fluorescence increased strongly after VEGF and only marginally after QK injection (Figure 8). Similar results were obtained when QK (three consecutive 1 μg doses in 1 mL instillations) or VEGF in equimolar amounts was topically applied onto the denuded meningeal surface in the bottom of the craniotomy window ($n = 4$ in both groups). Indeed, a significant leakage of fluorescent dextran into the brain parenchyma was observed when VEGF was locally instilled (NGL: 0.12 ± 0.03 vs 0.04 ± 0.02 , $p < 0.01$), whereas a similar application QK did not cause any effect on vessel permeability, as indicated by the fairly stable NGL values (NGL: 0.05 ± 0.03 vs 0.04 ± 0.02 , ns) (Figure 9). These data showed that, unlike VEGF, QK does not permeabilize pial vessels. Therefore, QK could represent an important therapeutic advancement for use in stroke compared to VEGF, which, at equimolar concentrations, promotes BBB permeabilization and hence the formation of brain edema.^{16,47}

It is unclear why QK retained the neuroprotective activity of VEGF while losing the ability to promote the permeabilization of the BBB. It should be considered, however, that a dissociation between neuroprotective and vessel permeabilizing effects was also observed with VEGF-E, a VEGF form produced by Orf viruses, which was explained as being a consequence of this growth factor not binding to VEGFR-1.⁴⁸ Some evidence has been reported, indeed, that VEGFR-1 takes part in vascular permeabilization,⁴⁹ although this effect is probably exerted in concert with VEGFR-2, which also controls vessel permeability.^{1,50} However, in contrast to VEGF-E, QK potentially activates not only VEGFR-2 but also VEGFR-1 *in vitro*.²⁷ An alternative hypothesis that could account for our findings relies on the evidence that although VEGFR-2 receptor activation is responsible for VEGF's angiogenic, neuroprotective, and permeabilizing effects,^{1,49} the transduction mechanisms involved diverge to some degree. Specifically, while Akt and MAPK activation are essential for neuroprotection and angiogenesis,^{1,50} vascular permeabilization is dependent on src^{51,52} and rac activation,⁵³ PKD1-mediated Syx phosphorylation,²² and NOS activation.^{52,54} Experimental evidence has been reported that these different angiogenic and vascular permeability pathways can be independently modulated. For instance, in cultured human umbilical vein endothelial cells (HUVEC), VEGF-induced angiogenesis is suppressed, whereas vascular permeabilization is enhanced when protein kinase C is inhibited.⁵⁵ Moreover, in porcine aortic endothelial cells stably expressing VEGFR-2, the PI3-K inhibitor, wortmannin, suppresses VEGF-induced rac activation with a much higher potency than ERK activation.⁵³ Importantly, structurally different VEGFR agonists may differentially affect the various VEGFR-2 transduction pathways, as reported in skin vessels, where VEGF₁₂₁ and

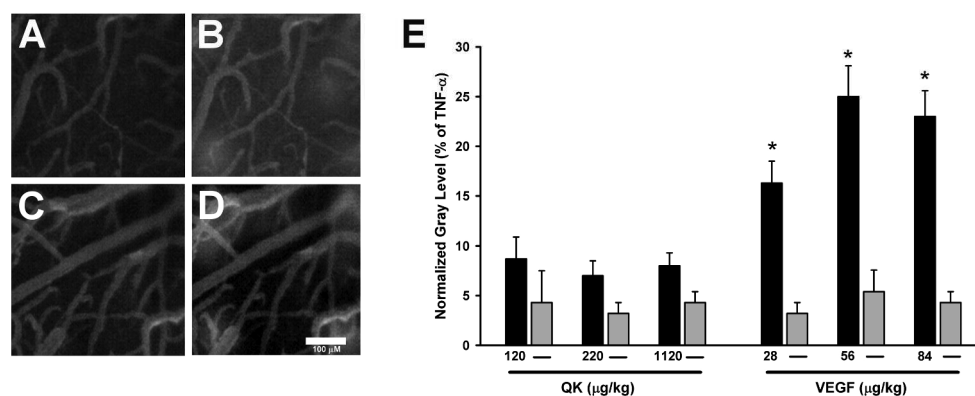


Figure 8. Intracarotid administration of VEGF but not QK causes vascular leakage in pial microcirculation. Images of pial microcirculation obtained before (A, C) and 5 min after (B, D) the intracarotid injection of 1.12 mg/kg QK and 84 mg/kg VEGF, respectively, in two rats previously injected with fluorescent dextran through the femoral artery. Note the marked increase in parenchymal fluorescence and the appearance of focal leakage of the dye after VEGF injection. (E) Quantification of experiments performed in different groups of rats receiving the intracarotid injection of increasing doses of QK or VEGF (black bars) or their vehicle (gray bars), as indicated. NGL data are expressed as the percent of values obtained after the iv injection of TNF- α (300 μ L of solution of 36 ng/mL injected in 3 min), a cytokine that causes maximal BBB leakage.⁶⁴ The black bars represent the mean \pm SEM of the values obtained in five different animals receiving either QK or VEGF, whereas the gray bars represent controls. * $p < 0.05$ vs control and QK (all doses).

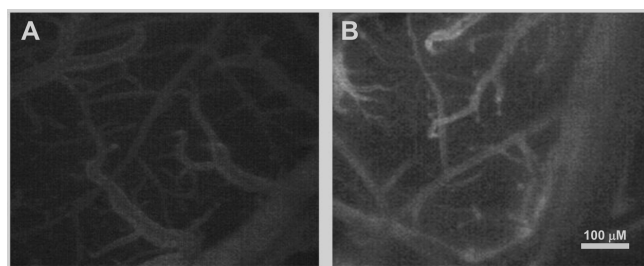


Figure 9. Topical administration of VEGF but not QK causes vascular leakage in pial microcirculation. (A, B) Images of the pial vascular bed obtained in a SD rat injected with fluorescent dextran 300 s after the local application of QK (A) or an equimolar amount of VEGF (B). This animal is representative of a group of 4. Note the diffuse fluorescence in the brain parenchyma in the VEGF, but not in the QK, injected rat. This suggests that VEGF, but not QK, increases vascular permeability in the brain.

VEGF₁₆₅ differentially activate src and the MAPK cascade.⁵⁶ Therefore, it is tempting to speculate that QK, which reproduces only part of the VEGF regions involved in receptor binding or regulation,⁵⁷ could selectively activate the neuroprotection transduction cascade and not the pathway responsible for vascular permeability.

In conclusion, we provided evidence that the VEGF-like peptide, QK, has neuroprotective activity in a rat model of stroke and that this effect occurs in the absence of vessel permeabilizing effects. Therefore, QK could be a promising alternative to VEGF for neuroprotection in stroke, which is further supported by its effectiveness when given not only by the icv route but also through minimally invasive administration routes, such as intranasally.

METHODS

Synthesis of QK and Its Fluorescein Conjugate. QK (acetyl-KLTWQELYQLKYKGI-amide) was synthesized as previously reported.²⁷ Briefly, the synthesis was carried out on solid phase by standard Fmoc (*N*-(9-fluorenyl)methoxycarbonyl) chemistry using a Rink Amide MBHA resin (Novabiochem, Billerica, MA, USA). The side chain of the N-terminal lysine was protected with a methyl-trytil group. To obtain a fluorescent QK derivative, 6-[fluorescein-5(6)-

carboxamido]hexanoic acid (Sigma-Aldrich, Milan, Italy) was coupled on solid phase to the peptidyl-resin after selective deprotection of this methyl-trytil group. QK and its fluorescent derivative were cleaved from the resin with trifluoroacetic acid, triisopropyl silane, and water (95:2.5:2.5) at room temperature for 3 h. Purity and identity of the peptides were assessed by HPLC and MALDI-TOF mass spectrometry.

Experimental Animals. All experiments were performed in male Sprague–Dawley rats weighing 250–270 g (Charles River, Calco, Italy). Rats were group caged on a 12 h light/dark cycle and had free access to food and water. The experimental protocol was approved by the Animal Care Committee of “Federico II”, University of Naples, Italy (CESA, Comitato Etico-Scientifico per la Sperimentazione Animale c/o Centro Servizi Veterinari). Animal housing and experimental procedures were performed according to the recommendations of the guidelines for the care and use of experimental animals of the European Community Council directive (86/609/EEC). All efforts were made to minimize animal suffering and to reduce the number of animals used in the experiments.

Design of the Study. We used two different experimental approaches to assess QK’s neuroprotective and vascular permeabilizing effects. To address the first point, experimental brain ischemia was induced by pMCAO, and QK was administered at different doses by different administration routes, as detailed below. The effect of the peptide on vessel permeability was evaluated by intravital pial microvessel videomicroscopy. The details of these techniques are reported below. In all experiments, simple randomization was used to allocate animals to the control or different intervention groups. All experiments were performed in a blinded manner, with different researchers performing drug administration or brain ischemia and analysis of behavioral/morphological data.

Permanent Middle Cerebral Artery Occlusion (pMCAO). pMCAO was performed as previously described.⁵⁸ Briefly, rats were deeply anesthetized with a gas mixture (4% sevoflurane in a 70% nitrous oxide/30% oxygen) delivered through a nose cone. Anesthesia was maintained with 2% sevoflurane. Under an operating stereomicroscope (Nikon SMZ800, Nikon Instruments, Florence, Italy), a 2 cm incision was made vertically between the orbit and the ear. The left lateral aspect of the skull was exposed by reflecting the temporal muscle, and a small window (diameter = 2 mm) was opened in the area corresponding to middle cerebral artery (MCA). Then, the MCA was permanently occluded as close as possible to its origin with a bipolar electrocauterizer (Diatermo MB122; G.I.M.A., Milan, Italy). Saline solution was applied during this procedure to prevent heat injury. Cortical cerebral blood flow was monitored with a laser-Doppler flowmeter (Periflux system 5000, Perimed, Milan, Italy) during the entire pMCAO procedure and

30 min thereafter. Rats in which cerebral blood flow did not drop below the threshold value of 70% of baseline after pMCAO were excluded from the study. During the entire surgical intervention, body temperature was maintained at 37.5 ± 0.5 °C with a thermostatic blanket (Homeothermic Blanket System, Harvard Apparatus, London, UK). Arterial blood gases were measured before and after ischemia through a catheter inserted into the femoral artery (Rapid lab 860; Chiron Diagnostic, Emeryville, CA, USA), and no differences were observed among the different experimental groups (data not shown).

Rats undergoing pMCAO were enrolled in the following experimental groups:

- (1) QK icv administration, pMCAO, sacrifice 3 days after surgery. Eighteen rats were randomized for the icv administration of either QK ($n = 8$) or its vehicle ($n = 10$). One animal was excluded from the control group because laser-Doppler flowmetry showed an insufficient drop in cerebral blood flow, whereas one rat from the QK group died before the time scheduled for sacrifice.
- (2) QK iv administration, pMCAO, sacrifice 3 days after surgery. Thirty nine rats were randomized in four groups to receive either QK (1.2, 12, and 120 $\mu\text{g}/\text{kg}$, $n = 11, 9$, and 10, respectively) or its vehicle ($n = 9$) intravenously 1 h after pMCAO. Nine rats (three in the 120 $\mu\text{g}/\text{kg}$ QK group and two in each of the other groups) were excluded from the experiment because of an insufficient decrease in cerebral blood flow determined by laser-Doppler flowmetry. Among the remaining 30 animals, eight died because of brain ischemia before the end of the experiment (two from the control group and three, two, and one from the groups receiving 1.2, 12, and 120 $\mu\text{g}/\text{kg}$ QK, respectively). Therefore, five rats in the control group and six, five, and six in the 1.2, 12, and 120 $\mu\text{g}/\text{kg}$ QK groups, respectively, completed the study.
- (3) QK intranasal administration, pMCAO, sacrifice 3 days after surgery. Fourteen rats were randomized in two groups to receive either intranasal QK (12 $\mu\text{g}/\text{kg}$) or vehicle 3 h after vessel occlusion. All of these animals completed the study because no insufficient blood flow drop by flowmetry or premature death was observed in either group.
- (4) QK intranasal administration, pMCAO, sacrifice 7 days after surgery. As in group 3, 14 animals were randomized in two groups to receive intranasally either QK ($n = 7$) or vehicle ($n = 7$). All of the animals enrolled completed the study.

QK Administration. QK was dissolved in 0.9% NaCl as a 60 $\mu\text{g}/\text{mL}$ (corresponding to about 300 μM) stock solution and stored at -80 °C in aliquots for later use.

The icv administration was performed through an implanted Alzet osmotic minipump (Durect, Cupertino, CA) as described elsewhere.⁵⁹ Pumps containing either QK (3 $\mu\text{g}/\text{mL}$, 1 $\mu\text{L}/\text{h}$) or vehicle were implanted 30 min before pMCAO, and QK administration began virtually at the time of pump implantation.

For iv administration, QK was injected in awake rats through the lateral tail vein after dipping the tail in warm water for about 1 min to dilate the vessels.

For intranasal administration, a total volume of 50 μL of the 60 $\mu\text{g}/\text{mL}$ QK solution, corresponding to about 3 μg for a 250 g rat (12 $\mu\text{g}/\text{kg}$), was instilled in the nasal cavities of awake rats as 10 μL aliquots introduced through a pipet tip alternatively in each of the nostrils with a 2 min interval between each administration.

Evaluation of Neurological Deficits. General and focal neurological deficits were evaluated according to Clark's scale.⁶⁰ Briefly, this grading scale assigns a numerical score to specific general (hair ruffling, position of ears, eye conditions, abnormal posture, decrease in spontaneous locomotor activity, occurrence of seizures) and focal (gait, body symmetry, climbing, turning behavior, front leg extension, compulsory circling, sensory response) neurological signs. The scores obtained for each of these signs are then added to calculate total general and focal neurological scores.

Evaluation of Ischemic Damage. The volume of the ischemic lesion was assessed 3 or 7 days after pMCAO, as described elsewhere.⁶¹ Briefly, rats were sacrificed by decapitation. Brains were quickly

removed, placed in ice-cold saline solution for 5 min, cut into 500 μM coronal slices with a Campden vibratome (Campden Instrument, 752M; UK), and stained with 2% triphenyl tetrazolium chloride (TTC). In all slices between +4.7 and -4.9 mm from bregma according to the Paxinos atlas, the infarcted region was identified as the white area after TTC staining and was measured with the image analysis software Image-Pro Plus (Image Pro Plus 4.1, Media Cybernetic, Rockville, MD, USA). The values obtained were used to calculate the volumes of each hemisphere and of the infarcted area, as detailed elsewhere.⁶¹

Confocal Immunofluorescence. Three hours after the intranasal administration of the fluorescein–QK conjugate (50 μL of a 75 $\mu\text{g}/\text{mL}$, i.e., approximately 300 μM , solution, given in five consecutive 10 μL administrations alternatively in each nostril), rats were deeply anesthetized with chloral hydrate (300 mg/kg ip) and transcardially perfused with 4% w/v paraformaldehyde in phosphate buffer. Coronal sections (60 μM thick) of the fixed brains were obtained with a cryostat (Microm HM 560, Thermo Scientific, France). Confocal analysis was performed as described elsewhere⁶² using a Zeiss LSM510 META/laser scanning confocal microscope. Single images were taken with an optical thickness of 0.7 μm and a resolution of 1024×1024 pixels.

Intravital Pial Microvessel Videomicroscopy. The effect of QK on pial brain microvessels was evaluated by intravital videomicroscopy, a method based on the visualization of pial vessels with a fluorescence microscope through a surgically prepared open cranial window.⁶³ Briefly, after inducing a deep anesthetization with α -chloralose (50 mg/kg of body weight, intraperitoneally) plus urethane (600 mg/kg of body weight, intraperitoneally), rats were tracheotomized and mechanically ventilated. Anesthesia was maintained with urethane alone (100 mg/kg of body weight, iv every hour). Both of the femoral arteries were catheterized: the left for blood pressure measurement and the right for the injection of fluorescent tracers. A cranial window (4 mm \times 5 mm) was drilled in the parietal bone (posterior, 1.5 mm to bregma; lateral, 3 mm to the midline), and the dura mater on its bottom was gently removed to expose pial microvessels. The anesthetized animal was then secured on the stage of a Leitz Orthoplan fluorescence microscope. A perfusion system was positioned into the cranial window to continuously superfuse the exposed brain surface with artificial cerebrospinal fluid heated at 37.0 ± 0.5 °C (119.0 mM NaCl, 2.5 mM KCl, 1.3 mM $\text{MgSO}_4 \cdot 7\text{H}_2\text{O}$, 1.0 mM NaH_2PO_4 , 26.2 mM NaHCO_3 , 2.5 mM CaCl_2 , and 11.0 mM glucose, equilibrated with 10.0% O_2 , 6.0% CO_2 , and 84.0% N_2 ; pH 7.38 ± 0.02). To visualize brain microvessels, dextran-bound fluorescein isothiocyanate (molecular weight 70 kDa) was injected through the right femoral artery (50 mg/100 g b.w., i.v. as 5 wt %/vol solution). Images were continuously acquired before and after QK or VEGF administration using a DAGE MTI 300RC low-light level digital camera connected to the microscope and recorded by a computer-based frame grabber (Pinnacle DC 10 plus, Avid Technology, MA, USA). Image analysis was performed offline using the MIP Image software system (CNR Institute of Clinical Physiology, Pisa, Italy). The effect of QK and VEGF on vessel permeability was evaluated by measuring the changes in extravascular fluorescence caused by the leakage of fluorescent dextran. The data were expressed as normalized gray levels (NGL), i.e., as the ratio between the averages of the gray levels measured in five different windows before and after QK or VEGF administration ($\text{NGL} = (I - I_r)/I_r$, where I_r is the average baseline gray level at the end of vessel filling with fluorescence and I is the same parameter at the end of QK or VEGF administration).

Statistical Analysis. Data were analyzed using Sigma Stat 3.5 software (Systat, San Jose, CA, USA), setting the threshold for statistical significance at $p < 0.05$. The Shapiro–Wilk test was used to assess whether data were normally distributed. Statistical comparisons of normally distributed data were performed with ANOVA followed by the Bonferroni *posthoc* test to correct for familywise errors. The significance of differences in general and focal neurological deficit scores was assessed with Kruskal–Wallis nonparametric ANOVA followed by Dunn's *posthoc* test.

AUTHOR INFORMATION

Corresponding Author

*Phone: +39 81-7462102; Fax: +39 81-7463323; E-mail: cataldi@unina.it.

Author Contributions

M.C., G.P., and L.d.A. designed the study. B.Z. and L.d.A. synthesized and purified the QK peptide. G.P., A.T., R.G., O.C., and A.V. performed pMCAO experiments. S.A. performed confocal microscopy experiments. D.L. and T.M. performed intravital pial microvessel videomicroscopy experiments. M.C., G.P., and L.d.A., C.P., L.A., G.d.R. analyzed the data and wrote the paper.

Funding

This work was supported by the following grants: PON 01_01602 from MIUR to L. Annunziato, PRIN2008, no. 200875WHMR from MIUR to L. D. D'Andrea, and FIRB no. RBRN07BMCT from MIUR to C. Pedone.

Notes

The authors declare no competing financial interest.

ACKNOWLEDGMENTS

The authors thank Vincenzo Grillo and Carmine Capitale for technical support.

REFERENCES

- (1) Ruiz de Almodovar, C., Lambrechts, D., Mazzone, M., and Carmeliet, P. (2009) Role and therapeutic potential of VEGF in the nervous system. *Physiol. Rev.* 89, 607–648.
- (2) Marti, H. J., Bernaudin, M., Bellail, A., Schoch, H., Euler, M., Petit, E., and Risau, W. (2000) Hypoxia-induced vascular endothelial growth factor expression precedes neovascularization after cerebral ischemia. *Am. J. Pathol.* 156, 965–976.
- (3) Beck, H., and Plate, K. H. (2009) Angiogenesis after cerebral ischemia. *Acta Neuropathol.* 117, 481–496.
- (4) Liman, T. G., and Endres, M. (2012) New vessels after stroke: postischemic neovascularization and regeneration. *Cerebrovasc. Dis.* 33, 492–499.
- (5) Schmidt, N. O., Koeder, D., Messing, M., Mueller, F. J., Aboody, K. S., Kim, S. U., Black, P. M., Carroll, R. S., Westphal, M., and Lamszus, K. (2009) Vascular endothelial growth factor-stimulated cerebral microvascular endothelial cells mediate the recruitment of neural stem cells to the neurovascular niche. *Brain Res.* 1268, 24–37.
- (6) Li, Q., Ford, M. C., Lavik, E. B., and Madri, J. A. (2006) Modeling the neurovascular niche: VEGF- and BDNF-mediated cross-talk between neural stem cells and endothelial cells: an in vitro study. *J. Neurosci. Res.* 84, 1656–1668.
- (7) Ma, Y., Zechariah, A., Qu, Y., and Hermann, D. M. (2012) Effects of vascular endothelial growth factor in ischemic stroke. *J. Neurosci. Res.* 90, 1873–1882.
- (8) Jin, K. L., Mao, X. O., and Greenberg, D. A. (2000) Vascular endothelial growth factor: direct neuroprotective effect in in vitro ischemia. *Proc. Natl. Acad. Sci. U. S. A.* 97, 10242–10247.
- (9) Matsuzaki, H., Tamatani, M., Yamaguchi, A., Namikawa, K., Kiyama, H., Matsuzaki, H., Tamatani, M., Yamaguchi, A., Namikawa, K., Kiyama, H., Vitek, M. P., Mitsuda, N., and Tohyama, M. (2001) Vascular endothelial growth factor rescues hippocampal neurons from glutamate-induced toxicity: signal transduction cascades. *FASEB J.* 15, 1218–1220.
- (10) Svensson, B., Peters, M., König, H. G., Poppe, M., Levkau, B., Rothermundt, M., Arolt, V., Kögel, D., and Prehn, J. H. (2002) Vascular endothelial growth factor protects cultured rat hippocampal neurons against hypoxic injury via an antiexcitotoxic, caspase-independent mechanism. *J. Cereb. Blood Flow Metab.* 22, 1170–1175.
- (11) Sun, Y., Jin, K., Xie, L., Childs, J., Mao, X. O., Logvinova, A., and Greenberg, D. A. (2003) VEGF-induced neuroprotection, neuro-

genesis, and angiogenesis after focal cerebral ischemia. *J. Clin. Invest.* 111, 1843–1851.

(12) Cataldi, M. (2013) The changing landscape of voltage-gated calcium channels in neurovascular disorders and in neurodegenerative diseases. *Curr. Neuropharmacol.* 11, 276–297.

(13) Annunziato, L., Pignataro, G., Boscia, F., Sirabella, R., Formisano, L., Saggese, M., Cuomo, O., Gala, R., Secondo, A., Viggiano, D., Molinaro, P., Valsecchi, V., Tortiglione, A., Adornetto, A., Scorziello, A., Cataldi, M., and Di Renzo, G. F. (2007) ncx1, ncx2, and ncx3 gene product expression and function in neuronal anoxia and brain ischemia. *Ann. N. Y. Acad. Sci.* 1099, 413–426.

(14) Annunziato, L., Cataldi, M., Pignataro, G., Secondo, A., and Molinaro, P. (2007) Glutamate-independent calcium toxicity: introduction. *Stroke* 38 (2 Suppl), 661–664.

(15) Senger, D. R., Galli, S. J., Dvorak, A. M., Perruzzi, C. A., Harvey, V. S., and Dvorak, H. F. (1983) Tumor cells secrete a vascular permeability factor that promotes accumulation of ascites fluid. *Science* 219, 983–985.

(16) Zhang, Z. G., Zhang, L., Jiang, Q., Zhang, R., Davies, K., Powers, C., Bruggen, Nv, and Chopp, M. (2000) VEGF enhances angiogenesis and promotes blood-brain barrier leakage in the ischemic brain. *J. Clin. Invest.* 106, 829–838.

(17) Yancopoulos, G. D., Davis, S., Gale, N. W., Rudge, J. S., Wiegand, S. J., and Holash, J. (2000) Vascular-specific growth factors and blood vessel formation. *Nature* 407, 242–248.

(18) Bates, D. O., and Curry, F. E. (1996) Vascular endothelial growth factor increases hydraulic conductivity of isolated perfused microvessels. *Am. J. Physiol.* 271, 2520–2528.

(19) Dobrogowska, D. H., Lossinsky, A. S., Tarnawski, M., and Vorbrodt, A. W. (1998) Increased blood-brain barrier permeability and endothelial abnormalities induced by vascular endothelial growth factor. *J. Neurocytol.* 27, 163–173.

(20) Roberts, W. G., and Palade, G. E. (1995) Increased microvascular permeability and endothelial fenestration induced by vascular endothelial growth factor. *J. Cell. Sci.* 108, 2369–2379.

(21) Weis, S. M., and Chesh, D. A. (2005) Pathophysiological consequences of VEGF-induced vascular permeability. *Nature* 437, 497–504.

(22) Ngok, S. P., Geyer, R., Liu, M., Kourtidis, A., Agrawal, S., Wu, C., Seerapu, H. R., Lewis-Tuffin, L. J., Moodie, K. L., Huvelde, D., Marx, R., Baraban, J. M., Storz, P., Horowitz, A., and Anastasiadis, P. Z. (2012) VEGF and Angiopoietin-1 exert opposing effects on cell junctions by regulating the Rho GEF Syx. *J. Cell Biol.* 199, 1103–1115.

(23) Schoch, H. J., Fischer, S., and Marti, H. H. (2002) Hypoxia-induced vascular endothelial growth factor expression causes vascular leakage in the brain. *Brain* 125 (Pt 11), 2549–2557.

(24) van Bruggen, N., Thibodeaux, H., Palmer, J. T., Lee, W. P., Fu, L., Cairns, B., Tumas, D., Gerlai, R., Williams, S. P., van Lookeren Campagne, M., and Ferrara, N. (1999) VEGF antagonism reduces edema formation and tissue damage after ischemic/reperfusion injury in the mouse brain. *J. Clin. Invest.* 104, 1613–1620.

(25) D'Andrea, L. D., Del Gatto, A., De Rosa, L., Romanelli, A., and Pedone, C. (2009) Peptides targeting angiogenesis related growth factor receptors. *Curr. Pharm. Des.* 15, 2414–2429.

(26) Diana, D., Basile, A., De Rosa, L., Di Stasi, R., Auriemma, S., Arra, C., Pedone, C., Turco, M. C., Fattorusso, R., and D'Andrea, L. D. (2011) β -hairpin peptide that targets vascular endothelial growth factor (VEGF) receptors: design, NMR characterization, and biological activity. *J. Biol. Chem.* 286, 41680–41691.

(27) D'Andrea, L. D., Iaccarino, G., Fattorusso, R., Sorriento, D., Carannante, C., Capasso, D., Trimarco, B., and Pedone, C. (2005) Targeting angiogenesis: structural characterization and biological properties of a de novo engineered VEGF mimicking peptide. *Proc. Natl. Acad. Sci. U. S. A.* 102, 14215–14220.

(28) Diana, D., Ziaco, B., Colombo, G., Scarabelli, G., Romanelli, A., Pedone, C., Fattorusso, R., and D'Andrea, L. D. (2008) Structural determinants of the unusual helix stability of a de novo engineered vascular endothelial growth factor (VEGF) mimicking peptide. *Chem. - Eur. J.* 14, 4164–4166.

- (29) Wiesmann, C., Fuh, G., Christinger, H. W., Eigenbrot, C., Wells, J. A., et al. (1997) Crystal structure at 1.7 Å resolution of VEGF in complex with domain 2 of the Flt-1 receptor. *Cell* 91, 695–704.
- (30) Finetti, F., Basile, A., Capasso, D., Di Gaetano, S., Di Stasi, R., Pascale, M., Turco, C. M., Ziche, M., Morbidelli, L., and D'Andrea, L. D. (2012) Functional and pharmacological characterization of a VEGF mimetic peptide on reparative angiogenesis. *Biochem. Pharmacol.* 84, 303–311.
- (31) Dudar, G. K., D'Andrea, L. D., Di Stasi, R., Pedone, C., and Wallace, J. L. (2008) A vascular endothelial growth factor mimetic accelerates gastric ulcer healing in an iNOS-dependent manner. *Am. J. Physiol. Gastrointest. Liver Physiol.* 295, G374–81.
- (32) Santulli, G., Ciccarelli, M., Palumbo, G., Campanile, A., Galasso, G., Ziaco, B., Altobelli, G. G., Cimmini, V., Piscione, F., D'Andrea, L. D., Pedone, C., Trimarco, B., and Iaccarino, G. (2009) In vivo properties of the proangiogenic peptide QK. *J. Transl. Med.* 7, 41.
- (33) Verheyen, A., Peeraer, E., Lambrechts, D., Poesen, K., Carmeliet, P., Shibuya, M., Pintelon, I., Timmermans, J. P., Nuydens, R., and Meert, T. (2013) Therapeutic potential of VEGF and VEGF-derived peptide in peripheral neuropathies. *Neuroscience* 244, 77–89.
- (34) Misra, A., and Kher, G. (2012) Drug delivery systems from nose to brain. *Curr. Pharm. Biotechnol.* 13, 2355–2379.
- (35) Thorne, R. G., and Frey, W. H., II (2001) Delivery of neurotrophic factors to the central nervous system: pharmacokinetic considerations. *Clin. Pharmacokinet.* 40, 907–946.
- (36) Gomez, D., Martinez, J. A., Hanson, L. R., Frey, W. H., 2nd, and Toth, C. C. (2012) Intranasal treatment of neurodegenerative diseases and stroke. *Front. Biosci., Scholar Ed.* 4, 74–89.
- (37) Chapman, C. D., Frey, W. H., 2nd, Craft, S., Danielyan, L., Hallschmid, M., Schiöth, and Benedict, C. (2013) Intranasal treatment of central nervous system dysfunction in humans. *Pharm. Res.* 30, 2475–2484.
- (38) Liu, X. F., Fawcett, J. R., Thorne, R. G., and Frey, W. H., II (2001) Non-invasive intranasal insulin-like growth factor-I reduces infarct volume and improves neurologic function in rats following middle cerebral artery occlusion. *Neurosci. Lett.* 308, 91–94.
- (39) Rodríguez Cruz, Y., Mengana Támos, Y., Muñoz Cernuda, A., Subirós Martínez, N., González-Quevedo, A., Sosa Testé, I., and García Rodríguez, J. C. (2010) Treatment with nasal neuro-EPO improves the neurological, cognitive, and histological state in a gerbil model of focal ischemia. *Sci. World J.* 10, 2288–300.
- (40) Zhao, H. M., Liu, X. F., Mao, X. W., and Chen, C. F. (2004) Intranasal delivery of nerve growth factor to protect the central nervous system against acute cerebral infarction. *Chin. Med. Sci. J.* 19, 257–61.
- (41) Ma, M., Ma, Y., Yi, X., Guo, R., Zhu, W., Fan, X., Xu, G., Frey, W. H., 2nd, and Liu, X. (2008) Intranasal delivery of transforming growth factor-beta1 in mice after stroke reduces infarct volume and increases neurogenesis in the subventricular zone. *BMC Neurosci.* 9, 117.
- (42) Yang, J. P., Liu, H. J., Wang, Z. L., Cheng, S. M., Cheng, X., et al. (2009) The dose-effectiveness of intranasal VEGF in treatment of experimental stroke. *Neurosci. Lett.* 461, 212–6.
- (43) Yang, J. P., Liu, H. J., Cheng, S. M., Wang, Z. L., Cheng, X., Yu, H. X., and Liu, X. F. (2009) Direct transport of VEGF from the nasal cavity to brain. *Neurosci. Lett.* 449, 108–111.
- (44) Danielyan, L., Schäfer, R., von Ameln-Mayerhofer, A., Buadze, M., Geisler, J., Klopfer, T., Burkhardt, U., Proksch, B., Verleysdonk, S., Ayturan, M., Buniatian, G. H., Gleiter, C. H., and Frey, W. H., 2nd (2009) Intranasal delivery of cells to the brain. *Eur. J. Cell Biol.* 88, 315–324.
- (45) Carmichael, S. T. (2005) Rodent models of focal stroke: size, mechanism, and purpose. *NeuroRx* 2, 396–409.
- (46) Lou, M., Blume, A., Zhao, Y., Gohlke, P., Deuschl, G., Herdegen, T., and Culman, J. (2004) Sustained blockade of brain AT1 receptors before and after focal cerebral ischemia alleviates neurologic deficits and reduces neuronal injury, apoptosis, and inflammatory responses in the rat. *J. Cereb. Blood Flow Metab.* 24, 536–47.
- (47) Manoonkitiwongsa, P. S., Schultz, R. L., McCreery, D. B., Whitter, E. F., and Lyden, P. D. (2004) Neuroprotection of ischemic brain by vascular endothelial growth factor is critically dependent on proper dosage and may be compromised by angiogenesis. *J. Cereb. Blood Flow Metab.* 24, 693–702.
- (48) Kiba, A., Sagara, H., Hara, T., and Shibuya, M. (2003) VEGFR-2-specific ligand VEGF-E induces non-edematous hyper-vascularization in mice. *Biochem. Biophys. Res. Commun.* 301, 371–377.
- (49) Vogel, C., Bauer, A., Wiesnet, M., Preissner, K. T., Schaper, W., Marti, H. H., and Fischer, S. (2007) Flt-1, but not Flk-1 mediates hyperpermeability through activation of the PI3-K/Akt pathway. *J. Cell. Physiol.* 212, 236–243.
- (50) Olsson, A. K., Dimberg, A., Kreuger, J., and Claesson-Welsh, L. (2006) VEGF receptor signalling - in control of vascular function. *Nat. Rev. Mol. Cell Biol.* 7, 359–371.
- (51) Suarez, S., and Ballmer-Hofer, K. (2001) VEGF transiently disrupts gap junctional communication in endothelial cells. *J. Cell. Sci.* 114, 1229–1235.
- (52) Weis, S. M., and Cheresh, D. A. (2005) Pathophysiological consequences of VEGF-induced vascular permeability. *Nature* 437, 497–504.
- (53) Eriksson, A., Cao, R., Roy, J., Tritsarlis, K., Wahlestedt, C., Dissing, S., Thyberg, J., and Cao, Y. (2003) Small GTP-binding protein Rac is an essential mediator of vascular endothelial growth factor-induced endothelial fenestrations and vascular permeability. *Circulation* 107, 1532–1538.
- (54) Lal, B. K., Varma, S., Pappas, P. J., Hobson, R. W., 2nd, and Durán, W. N. (2001) VEGF increases permeability of the endothelial cell monolayer by activation of PKB/akt, endothelial nitric-oxide synthase, and MAP kinase pathways. *Microvasc. Res.* 62, 252–262.
- (55) Spyridopoulos, I., Luedemann, C., Chen, D., Kearney, M., Chen, D., Murohara, T., Principe, N., Isner, J. M., and Losordo, D. W. (2002) Divergence of angiogenic and vascular permeability signaling by VEGF: inhibition of protein kinase C suppresses VEGF-induced angiogenesis, but promotes VEGF-induced, NO-dependent vascular permeability. *Arterioscler., Thromb., Vasc. Biol.* 22, 901–906.
- (56) Zhang, Y., Furumura, M., and Morita, E. (2008) Distinct signaling pathways confer different vascular responses to VEGF 121 and VEGF 165. *Growth Factors* 26, 125–131.
- (57) Keyt, B. A., Nguyen, H. V., Berleau, L. T., Duarte, C. M., Park, J., Chen, H., and Ferrara, N. (1996) Identification of vascular endothelial growth factor determinants for binding KDR and FLT-1 receptors. Generation of receptor-selective VEGF variants by site-directed mutagenesis. *J. Biol. Chem.* 271, 5638–5646.
- (58) Tortiglione, A., Minale, M., Pignataro, G., Amoroso, S., Di Renzo, G., and Annunziato, L. (2002) The 2-oxopyrrolidinacetamide piracetam reduces infarct brain volume induced by permanent middle cerebral artery occlusion in male rats. *Neuropharmacology* 43, 427–433.
- (59) Pignataro, G., Gala, R., Cuomo, O., Tortiglione, A., Giaccio, L., Castaldo, P., Sirabella, R., Matrone, C., Canitano, A., Amoroso, S., Di Renzo, G., and Annunziato, L. (2004) Two sodium/calcium exchanger gene products, NCX1 and NCX3, play a major role in the development of permanent focal cerebral ischemia. *Stroke* 35, 2566–2570.
- (60) Clark, W. M., Lessov, N. S., Dixon, M. P., and Eckenstein, F. (1997) Monofilament intraluminal middle cerebral artery occlusion in the mouse. *Neurol. Res.* 19, 641–648.
- (61) Cuomo, O., Rispoli, V., Leo, A., Politi, G. B., Vinciguerra, A., di Renzo, G., and Cataldi, M. (2013) The antiepileptic drug levetiracetam suppresses non-convulsive seizure activity and reduces ischemic brain damage in rats subjected to permanent middle cerebral artery occlusion. *PLoS One* 8, e80852.
- (62) Boscia, F., Gala, R., Pannaccione, A., Secondo, A., Scorziello, A., Di Renzo, G., and Annunziato, L. (2009) NCX1 expression and functional activity increase in microglia invading the infarct core. *Stroke* 40, 3608–3617.
- (63) Lapi, D., Vagnani, S., Pignataro, G., Esposito, E., Paterni, M., and Colantuoni, A. (2012) Rat Pial Microvascular Responses to Transient Bilateral Common Carotid Artery Occlusion and Reperfusion: Quercetin's Mechanism of Action. *Front. Physiol.* 3, 99.
- (64) Mayhan, W. G. (2002) Cellular mechanisms by which tumor necrosis factor-alpha produces disruption of the blood-brain barrier. *Brain Res.* 927, 144–52.